Firefly Algorithm-assisted ANN Modelling approach for predicting Rhodamine B adsorption from simulated wastewater using sewage sludge biochar/ silica gel composite

Neelaambhigai Mayilswamy
Department of Metallurgical and Materials Engineering
Defence Institute of Advanced Technology (DU)
Girinagar, Pune- 411025, Maharashtra, India
neelaambhigai.mayilswamy@gmail.com

Balasubramanian Kandasubramanian*
Department of Metallurgical and Materials Engineering
Defence Institute of Advanced Technology (DU)
Girinagar, Pune- 411025, Maharashtra, India
meetkbs@gmail.com
ORCID: https://orcid.org/0000-0003-4257-8807

Satkirti Chame
Department of Chemical Engineering
Institute of Chemical Technology
Mumbai, Marathwada Campus, Jalna, Maharashtra, India
satkirti002@gmail.com

Tushar Warjurkar
Department of Chemical Engineering
Institute of Chemical Technology
Mumbai, Marathwada Campus, Jalna, Maharashtra, India
tusharwarjurkar.2003@gmail.com

doi: https://doi.org/10.37285/bsp.SACAD2025.62

***Abstract*— This research work articulates the development of sewage sludge biochar/silica gel composites (SSB/SiO_2-W: non-indicating, SSB/SiO_2-B: indicating) for the detoxification of Rhodamine B (RhB)-laden wastewater, in conjunction with Artificial Neural Network (ANN) Modelling. SSB/SiO_2-B adsorbent demonstrated slightly higher adsorption capacity values in contrast with SSB/SiO_2-W, with corresponding utmost adsorption capacities of 8.28 mg/g, and 8.43 mg/g, respectively, at preliminary dye concentrations of 15 ppm. Dye removal adhered to the Pseudo-second order kinetics, and aligned closely with the Langmuir isotherm model, connoting a chemisorption based-rate limiting step, and homogeneous single-layer dye adsorption, respectively. The ANN model developed via the Levenberg Marquardt Backpropagation Algorithm optimized by Firefly Algorithm (FA), for prognosticating RhB adsorption capacities manifested greater correlation (R:- SSB/SiO_2-W: 0.9898, SSB/SiO_2-B: 0.9811), and determination coefficients (R^2:- SSB/SiO_2-W: 0.9955, SSB/SiO_2-B: 0.9917), along with lower mean square errors (SSB/SiO_2-W: 0.1387, SSB/SiO_2-B: 0.2919), substantiating a significant correlation between the experimental and ANN predicted responses. This work established sewage sludge biochar/silica gel composites as highly efficacious, and economical adsorbents for RhB dye decolorization.**

Keywords*—ANN Modelling, Firefly Algorithm, Biochar/silica gel composite, Rhodamine B, Adsorption thermodynamics, Regeneration studies.

I. INTRODUCTION

Effluents generated from diverse sectors encompassing the textile, plastic, paper, pulp, cosmetics, and rubber, serve as the predominant sources of dye pollution in aquatic ecosystems. Roughly 8 x 10^5 tonnes of dyes are produced per annum, with 20% discharged into industrial wastewater and 12% released during processing stages. Rhodamine B belongs to the Xanthene family of fluorescent dyes and is widely employed as colorants in the textile, and paper processing sectors, for dyeing jute, silk, cotton, leather, and wool. It is also employed as chelating ligand, and cytometry, fluorescent microscopy analysis, etc. [1]. This dye is associated with carcinogenic, teratogenic, and developmental toxicity impacts on the human, and animal health. Hence, dye removal from effluents is imperative to safeguard both environmental and human health [1]. The customarily utilized strategies aimed at addressing dye wastewater pollution encompass ion exchange, membrane filtration, precipitation, sedimentation, adsorption coagulation and flocculation, etc. Amongst the multitudinous dye remediation methodologies, adsorption is the most preferable, ascribable to intrinsic advantages related to higher process efficacy, simplistic operation, simplicity of design, and facile extraction from water. Activated carbon generated from coal is extensively used for dye decolorization from aqueous matrices. Contemporarily, researchers are scrutinizing biochar-derived adsorbents for the cost-efficient, and eco-safe detoxification of dye wastewater. Biochar as carbonaceous substances, possessing greater porosity, total pore volume, specific surface area, plenteous surface functionalities, tunable characteristics, and regenerability serve as low-cost alternatives to conventional adsorbents for environmental remediation [2].

It is estimated that sewage sludge generation would rise from 53 million tonnes to 160 million tonnes, in line with worldwide wastewater production. Landfilling or incineration of sludge-based wastes ensues in secondary pollution concerns, and sludge handling, and management prices amount to 20-60% of the overall operating cost [3]. The pyrolysis of sewage sludge into biochar adsorbents for the sustainable detoxification of toxic dyes from effluents, solves dual predicaments associated with sludge disposal, and environmental remediation. This strategy facilitates the adoption of resource recovery and waste minimization principles, aligning with the targets set by the United Nations Sustainable Development Goals (SDGs) [3]. The physicochemical properties of biochars for dye adsorption can be enhanced via physical or chemical activation. Among various chemical activation methods, biochar functionalization with silica imparts good mechanical stability, introduces hierarchic porous frameworks, and is characterized by copiousness, and cost-effectiveness, despite possessing lower adsorption capacities [4]. Integrating the expedient characteristics of biochar and silica to generate composites would be favorable for enhancing dye removal efficacy from effluents.

Modeling and simulation of effluent treatment phenomena are essential for process optimization, and ensuring reduction in usage of chemicals. The interrelations between the predictors, and responses involved in dye adsorption mechanism are intricate to predict using the traditional mathematical models. ANN modelling is customarily utilized to study non-linear correlations between the responses and predictors, contingent with the principle of biological neurons. In contrast with the conventional mathematical models, ANN exhibits multitudinous benefits such as process flexibility, effective operation with noisy data, and the ability to model any type of non-linear correlations, without adherence to established conventions [5].

In light of existing research, few studies have explored biochar/silica gel composites for the adsorption of toxic metal ions from aqueous matrices [6]. However, no preceding research has reported a comparative investigation of sewage sludge biochar functionalized with two distinct grades of silica gel- blue (indicating), and white (non-indicating) for RhB dye adsorption for simulated effluents, at dye concentrations approaching the maximum permissible limit of dye (0.14 ppm). This research introduces, for the first time, the use of indicator-grade silica in SSB functionalization for RhB uptake, coupled with Firefly Algorithm–optimized ANN modeling to predict adsorption performance. Adsorption kinetics, isotherms, thermodynamics, pH and adsorbent dose impacts, regeneration, and a Pearson matrix heatmap are also elucidated, imparting a novel experimental-computational insight into dye adsorption performance.

II. METHODOLOGICAL FRAMEWORK

A. Biochar precursors and chemicals utilized

Sewage sludge was obtained from a municipal wastewater treatment facility situated in Bopodi, Pune, India. The harvested biosolid was subjected to drying at 100°C for 24 hours in an oven to eliminate residual water content. The desiccated sludge was processed into a powder, and subsequently sieved to isolate fine particulate matter traversing between 90-150 microns. Silica gel (SiO_2): white - W (non-indicating, CAS No.: 112926-00-8), and blue - B (self-indicating- incorporates cobalt as an indicator, CAS No.: 112926-00-8) was purchased from SRL Pvt. Ltd., Maharashtra, India. Rhodamine B dye (Molecular formula: $C_{28}H_{31}ClN_2O_3$, M.W.: 479.01 g/mol) was acquired from SRL Pvt. Ltd., Maharashtra, India. Sodium hydroxide pellets (≥ 98% purity), and hydrochloric acid (AR grade - 35.4%) were supplied by Loba Chemie Pvt. Ltd., Maharashtra, India, and Sigma-Aldrich, Karnataka, India, respectively. Glacial acetic acid (extra pure - 99.5%) was purchased from Loba Chemie Pvt. Ltd., Maharashtra, India.

B. Fabrication of sewage sludge biochar (SSB)/ silica gel composites

Synthesis of sewage sludge biochar/ silica gel (SiO_2) composites was performed by traditional pyrolytic conversion of sewage sludge biomass into biochar, succeeded by chemical functionalization with two different grades of SiO_2 – white (non-indicating), and blue (non-indicating). 15 of desiccated sewage sludge underwent pyrolysis in a tube furnace at 500 °C, for 60 minutes, at a heating rate of 10 °C/min, in a controlled atmosphere of nitrogen gas. 2.5 g of the fabricated SSB, and 0.25 g of silica gel (10:1 ratio – biochar: silica gel) are dispersed in water, and acetone respectively for one hour using via ultrasonication. The two separation solutions were then mixed and subjected to overnight stirring on a magnetic stirrer for 15 hours. The activated biochar is desiccated in a hot air oven at 120 °C for 24 hours. The dried sample is exposed to subsequent pyrolysis reaction at 500 °C for 120 minutes, at a heating rate of 5 °C/min, in nitrogen environment to yield biochar/silica gel composites, designated as SSB/SiO_2-W, SSB/SiO_2-B.

C. Characterization of biochar composites

The molecular functional groups found in the biochar/silica gel composites pre-, and post-RhB decolorization were examined using Fourier Transform Infrared Spectroscopy (FTIR). Infrared spectral data were acquired with the aid of the Bruker-Alpha 200630 instrument, covering a wavelength spectrum from 4000 to 400 cm^{-1}. The surface morphological changes of the biochar composites pre-, and post-RhB decolorization was investigated through Scanning electron microscopy (SEM) analysis employing the Carl-Zeiss GmbH Field-Emission SEM instrument. Energy dispersive X-ray (EDX) spectroscopy was performed on the biochar/silica gel composites before, and after dye decolorization, to comprehend the elemental constitution, and mapping (Oxford XMAX N50 EDX detector). The specific surface area of the biochar/silica gel composites, pre-dye removal was estimated through the Brauner-Emmett-Teller (BET) method, determined through nitrogen gas adsorption and desorption across different relative pressure values (Quantachrome St1 on NOVA touch 4LX), with prefatory vacuum degassing at 300 °C for three hours. The Barrett-Joyner-Halenda (BJH) technique was employed to estimate the pore volume, and diameter of the adsorbents before dye uptake.

D. Batch adsorption studies of RhB dye

Rhodamine B batch adsorption assays were implemented to explore the adsorption properties of SSB/SiO_2 composite. RhB solutions of different working concentrations were prepared through serial dilution approach of the 1000 ppm stock solution. 20 mg of the biochar/silica gel composites were added to 20 mL of 15 ppm RhB dye solution in conical flasks. The conical flasks containing the adsorbent-adsorbate mixtures were then placed on the orbital shaker (Bio Technics India, Model: BTI-05) and shaken at 200 rpm for a duration of six hours. Post-equilibration, the adsorbent-adsorbate mixtures were processed in a centrifuge operating at 14,500 rpm over a 15-minute interval (Eppendorf Centrifuge Model: 5430 R), to segregate the biochar composite from the RhB solution. An aliquot of the post-adsorption mixture was analyzed for its spectral absorbance readings at λ_{max} = 554 nm (maximal peak absorption wavelength of RhB dye) using UV-visible-spectroscopy (UV 3200 Labindia double beam UV spectrophotometer). The effect of distinct variables on RhB detoxification employing the biochar/silica gel composites (SSB/SiO_2-W, B) was analyzed, encompassing contact time-adsorption kinetics (15 min – 6 hr), pH (2 – 12), temperature-adsorption thermodynamics (25 - 45°C), biochar/silica gel dosage (10 – 100 mg), and preliminary dye concentration-adsorption isotherm (0.14 – 15 ppm). The adsorption studies associated with influence of solution pH values on dye adsorption were executed by modifying the solution pH utilizing 0.1 N HCl or NaOH solutions. All the adsorption experiments were replicated, and implemented synchronously to reduce the experimental inaccuracies. The equilibrium adsorption capacity, and RhB removal efficacy employing the SSB/SiO_2 composites were determined using the following equations (Equations 1-2) [7]:-

$$q_e = \frac{(C_o - C_e)V}{m} \quad (1)$$

$$R = \frac{(C_o - C_e)}{C_o} \times 100 \quad (2)$$

Where,
q_e = Equilibrium dye adsorption capacity of biochar silica-gel composite (mg/g);
R = RhB removal efficacy (%);
C_e = RhB dye concentration at equilibrium (ppm);
C_o = Starting concentration of RhB (mg/L);
m = Mass of biochar composite used (g);
V= Overall volume of dye solution (L).

E. Adsorption isotherms, kinetics, and thermodynamics

1) Adsorption kinetics

The experimental data obtained from the time-dependent behavior of RhB adsorption using the sewage sludge biochar/silica gel composites was modelled with Pseudo-first order (PFO), and Pseudo-second order (PSO) kinetic models, to ascertain the adsorption rate, and governing mass transfer mechanisms. The mathematical expressions contemplating the aforestated linear adsorption kinetic models are mentioned below (Equations 3-4) [8,9]:-

PFO kinetic model:- $ln(q_e - q_t) = lnq_e - k_1 t$ (3)

PSO kinetic model:- $\frac{t}{q_t} = \frac{1}{k_2 q_e^2} + \frac{1}{q_e} t$ (4)

Where,
q_t**:** Quantity of dye adsorbed at time t (mg/g); q_e: Maximal RhB adsorption capacity of biochar composite at equilibrium (mg/g); k_1**:** PFO model rate constant (min^{-1}); k_2**:** PSO model rate constant (g/(mg·min)).

2) Adsorption isotherms

The outcomes of RhB adsorption experiments based on varying initial dye concentration was modelled with Freundlich, and Langmuir adsorption isotherm models, to comprehend the utmost adsorption capacity, and plausible mechanisms responsible for the dye decolorization phenomenon. The mathematical equations associated of these adsorption isotherms are outlined below (Equations 5-6) [10]:-

Freundlich model:- $lnq_e = \frac{1}{n} lnC_e + lnK_F$ (5)

Langmuir model:- $\frac{C_e}{q_e} = \frac{1}{K_L q_{max}} + \frac{C_e}{q_{max}}$ (6)

Where,
C_e**:** RhB dye concentration at equilibrium (mg/L); q_e: Amount of RhB dye adsorbed per unit mass of biochar composite at equilibrium (mg/L); k_F**:** Freundlich adsorption isotherm constant (L/g); $\frac{1}{n}$: Non-dimensional exponent; q_{max}**:** Utmost mono-layered dye adsorption capacity (mg/g); k_L**:** Langmuir isotherm constant (L/mg).

3) Adsorption thermodynamics

The thermodynamic study of RhB decolorization facilitates the investigation of distinct properties and the partial adsorption characteristics of the biochar/silica gel composite–RhB dye system. The various significant thermodynamics parameters including the free enthalpy change (ΔH°), free entropy change (ΔS°), and Gibb's free energy change values (ΔG°), are computed through Van't Hoff's equation (Equations 7-8) [7].

$$k_d = \frac{q_e}{C_e} \quad (7)$$

$$lnk_d = \frac{\Delta S^o}{R} - \frac{\Delta H^o}{RT} \quad (8)$$

ΔG° values are computed through the following equation (Equation 9):-

$$\Delta G^o = \Delta H^o - T\Delta S^o \quad (9)$$

Where,
ΔS^o = Free entropy change;
ΔH^o = Free enthalpy change;
ΔG^o = Gibb's free energy change;
R = Universal gas constant (8.314 J/mol/K);
k_d= Distribution coefficient.

In accordance with equation 8, the values of ΔS°, and ΔH° were estimated from the correspondent intercept, and slope values obtained through linear regression, based on a plot of lnk_d vs. *1/T*. ΔG^o values are computed by solving Equation 9 with the calculated ΔS^o, and ΔH^o values.

F. Desorption and regeneration analysis

The regeneration characteristics of the spent biochar/silica gel composites were studied to understand their potential for industrial-scale wastewater treatment applications. To examine the regeneration potential of the dye-loaded biochar composites, sequential adsorption-desorption experiments were carried out using 0.1N acetic acid solution. Initially, 1.5 g of the SSB/SiO_2-W,B adsorbents were shaken with 750 mL RhB solution (concentration: 15 ppm) for 6 hours. Post-attainment of equilibrium, the decanted dye solution was eliminated, and the spent adsorbents were rinsed with double-distilled water to eradicate any residuary unadsorbed dye moieties. The recycled adsorbents were segregated from the dye solution, and desiccated in the oven at 80 °C overnight, for consequential RhB dye uptake studies via the aforestated protocol for 3 cycles of adsorption-desorption.

G. *Predictive modelling of RhB dye removal using the FA-optimized ANN framework*

In this research work, ANN modelling was performed to prognosticate the dye adsorption capacities employing biochar/silica gel composites via the Levenberg Marquardt Backpropagation (LM) Algorithm, using MATLAB 2023a software. The experimental dataset consisting of 33 data points was stochastically partitioned into 70% (23 data points) for training, 15% (5 data points) for validation, and 15% (5 data points) for testing, for the ANN modelling purpose. Solution temperature, pH, contact duration, biochar composite dose, and preliminary adsorbate concentration were selected as the predictors, while adsorption capacity was considered the response in the ANN Modelling phenomenon, with the hidden layer neurons being enumerated using Firefly Algorithm, an evolution-inspired optimization methodology predicated on the flashing behavior of fireflies. FA was selected for ANN optimization owing to its superior convergence speed, ability to avoid local minima, capability to handle multimodal problems, and simplicity of implementation over other evolutionary algorithms such as Differential Evolution, Particle Swarm Optimization, and Genetic Algorithm. The optimal hidden layer neurons evaluated using FA, was subsequently processed with the LM Backpropagation Algorithm, employing 'purelin" transfer function for response, and "tansig" transfer function for predictors, respectively. The predictive capability of the ANN model was gauged by evaluating specific statistical metrics, enlisted below (Equations 10-13) [11]:-

$$\text{Mean square error, } MSE = \frac{\sum_{i=1}^{N}(y_{m,i}-y_{e,i})^2}{n} \quad (10)$$

$$\text{Mean absolute error, } MAE = \frac{\sum_{i=1}^{n}|y_{m,i}-y_{e,i}|}{n} \quad (11)$$

$$\text{Determination coefficient, } R^2 = 1 - \frac{\sum_{i=1}^{N}(y_{m,i}-y_{e,i})^2}{\sum_{i=1}^{N}(y_{e,i}-y_{m\,av})^2} \quad (12)$$

$$\text{Root mean square error, } RMSE = \sqrt{\frac{\sum_{i=1}^{N}(y_{m,i}-y_{e,i})^2}{n}} \quad (13)$$

Where,
n = Sample size in ANN Modelling;
$y_{e,i}$ = Experimental dye adsorption capacity values;
$y_{m,i}$ = ANN prognosticated adsorption capacity values;
$y_{m\,av}$ = Mean value of ANN model's predictions.

H. *Visualization of pearson correlation matrix via heatmap*

A color-coded map of the Pearson correlation matrix was developed with the aid of PyCharm Professional 2012.2 version of Python programming language, to probe the associations that exist between the discrete, and paired input, and output values. The correlation coefficient (r) values, spanning between -1 to +1, were computed for each pairwise correlation.

III. RESULTS AND DISCUSSION

A. *Characterization of SSB/SiO$_2$ composite*

Fig. 1. (a), (b) represents the FTIR spectra of SSB/SiO$_2$-W, and SSB/SiO$_2$-B composites pre-, and post-RhB decolorization to understand the modifications in the surface functionalities, with dye adsorption. The FTIR spectrum of SSB/SiO$_2$-W manifests prominent FTIR peaks around 1597 cm^{-1}, 1366 cm^{-1}, 1076 cm^{-1}, 800 cm^{-1}, 754 cm^{-1}, and 459 cm^{-1}, cognate with C=C aromatic skeletal vibrations, O-H bending vibrations associated with phenolic/ carboxylic group, Si-O-Si stretching vibrations, presence of SiO$_4$ tetrahedron, Si-C stretching, and Si-O stretching vibrations, respectively. Post-RhB adsorption, FTIR peak shifts were observed from 1597 to 1591 cm^{-1}, 1076 to 1070 cm^{-1}, 754 to 759 cm^{-1}, 459 to 441 cm^{-1}, indicating the intervention of C=C aromatic vibrations, Si-O-Si stretching, Si-C stretching, and Si-O stretching vibrations in the dye uptake phenomenon through π-π interactions, surface complexation, and electrostatic interactions. Furthermore, the FTIR peak at 1366 cm^{-1} corresponding to O-H bending vibrations disappeared, accompanied by the emergence of a new peak at 668 cm^{-1}, contingent with C-H bonding, substantiating successful RhB uptake onto the SSB/SiO$_2$-W adsorbent **(Fig. 1 (a))** [12,13]. The FTIR spectrum of SSB/SiO$_2$-B adsorbent demonstrated peaks consistent with Si-O-Si stretching, C=C aromatic vibrations, C-H group axial deformation, -CH$_2$ group, Si-O stretching, Si-C stretching, and the existence of SiO$_4$ tetrahedron ring at wavenumbers around 1093 cm^{-1}, 1597 cm^{-1}, 2888 cm^{-1}, 1407 cm^{-1}, 455 cm^{-1}, 754 cm^{-1}, and 800 cm^{-1}, respectively. After RhB decolorization, FTIR peak shifts were observed from 1597 to 1590 cm^{-1}, 1093 to 1081 cm^{-1}, 754 to 749 cm^{-1}, evidencing the participation of C=C aromatic vibrations, Si-O-Si stretching, and SiO$_4$ tetrahedron ring in the dye uptake process via π-π interactions, and surface complexation. This was accompanied by the loss of the IR peak at 2888 cm^{-1}, in conjunction with the appearance of an additional peak at 667 cm^{-1}, contingent with C-H bonding, confirming successful RhB adsorption into the SSB/SiO$_2$-B composite [14,15] **(Fig. 1. (b))**.

Fig. 1. (c), (d) exemplifies the BET N$_2$-adsoprtion desorption isotherm plots of SSB/SiO$_2$-W, SSB/SiO$_2$-B adsorbents before RhB uptake. Contingent with the IUPAC, both the biochar composites exhibited type-IV BET isotherms, distinctive of mesoporous adsorbents, involving nitrogen condensation phenomenon [16]. SSB/SiO$_2$-W demonstrated a moderately greater surface area (40.10 m^2/g) in contrast with SSB/SiO$_2$-B (33.04 m^2/g). The total pore volumes of the biochar composites enumerated through the BJH method were found to be 0.13 cm^3/g, and 0.08 cm^3/g, respectively **(Fig. 1. (e), (f))**. The pore diameters of the biochar/silica gel composites ranged between 2-50 nm, thereby substantiating their mesoporous nature **(TABLE I.)**. SSB/SiO$_2$-B adsorbent albeit possessing a lower pore volume, specific surface area, and pore diameter when contrasted with SSB/SiO$_2$-W demonstrated slightly greater q_{max} values. The structural dimensions of RhB dye moieties were of the order of 10.9 Å x 14.4 Å x 5 Å. Considering the dimensions of RhB dye, it is more likely to occupy an adsorbent with a pore diameter of 3.83 nm (SSB/SiO$_2$-B) more rapidly than it would be in

adsorbents with more broader pore diameters via pore filling mechanism.

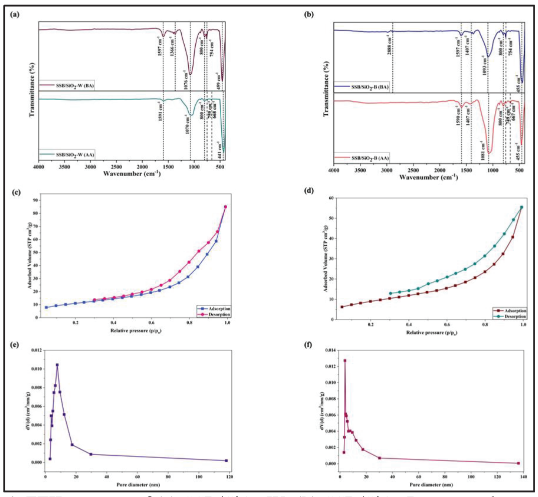

Fig. 1. FTIR spectra of **(a)** SSB/SiO_2-W, **(b)** SSB/SiO_2-B, pre- and post-dye uptake; BET N_2-adsorption desorption isotherm of **(c)** SSB/SiO_2-W, **(d)** SSB/SiO_2-B, prior to RhB adsorption; BJH plot of **(e)** SSB/SiO_2-W, **(f)** SSB/SiO_2-B, before RhB decolorization.

TABLE I. SURFACE PROPERTIES OF BIOCHAR/SILICA GEL COMPOSITES PRIOR TO RHB DYE DECOLORIZATION.

Biochar/composite	Pore volume (cm^3/g)	Surface area (m^2/g)	Pore diameter (nm)
SSB/SiO_2-W	0.13	40.10	7.74
SSB/SiO_2-B	0.08	33.04	3.83

The SEM images of SSB/SiO_2-W, and SSB/SiO_2-B composites prior to dye removal from simulated wastewater exhibited an irregular, porous, and rough surface texture which is characteristic of biochar/silica gel composites **(Fig. 2. (a), (c))**. The mesopores present in the biochar composite possess reasonable specific surface area conducive for dye adsorption. Post-RhB uptake, the adsorbent surface seems to be relatively smoother, and more compact indicating that the pore of the biochar composites have been partially filled with the dye moieties **(Fig. 2. (b), (d))**. EDX analysis of both the biochar composites signified the presence predominant amounts of carbon (SSB/SiO_2-W: 56.50 wt.% , SSB/SiO_2-B: 72.60 wt.%), and oxygen (SSB/SiO_2-W: 28.18 wt.%, SSB/SiO_2-B: 20.33 wt.%), followed by silicon (SSB/SiO_2-W: 6.04 wt.% , SSB/SiO_2-B: 3.70 wt.%), and trace amounts of other elements such as iron, magnesium, aluminium, etc. **(Fig. 2. (e), (g))**. The appearance of Si in significant wt.% confirms successful functionalization of sewage sludge biochar with silica gel. After RhB uptake, a diminution in the carbon composition, and increment in the oxygen composition was ascertained, along with the emergence of nitrogen atoms from RhB dye, revealing that the dye was effectively sequestered onto the biochar composites **(Fig. 2. (f), (h))** [17].

B. RhB batch adsorption studies employing SSB/SiO_2 composites

1) Adsorption kinetics, isotherm, and thermodynamics

The RhB dye adsorption onto SSB/SiO_2-W, B composites was most accurately represented by the PSO kinetic model, as it exhibited a determination coefficient (R^2) value demonstrating proximity to one, relative to the PFO model **(Fig. 3. (a), (b))**. This signifies that the rate limiting step of the dye decolorization phenomenon was chemisorption, pertaining to the exchange/ delocalization of electrons within the adsorbent-adsorbate system. The adsorption isotherm studies involving RhB decolorization using both biochar composites fitted well with the Langmuir adsorption isotherm, as evidenced by higher R^2 values compared to the Freundlich adsorption isotherm **(Fig. 3. (c), (d))**. This indicates that RhB sequestration from dye-contaminated effluent was homogeneous, and involved mono-layered dye adsorption. SSB/SiO_2-B (q_m: 8.4317 mg/g) exhibited slightly greater utmost dye adsorption capacity values compared to SSB/SiO_2-W (q_m: 8.2781 mg/g). The time-dependent adsorption patterns, and isotherm characteristics regulating RhB discoloration from simulated wastewater utilizing the biochar/silica gel composites are enlisted in **TABLE II**.

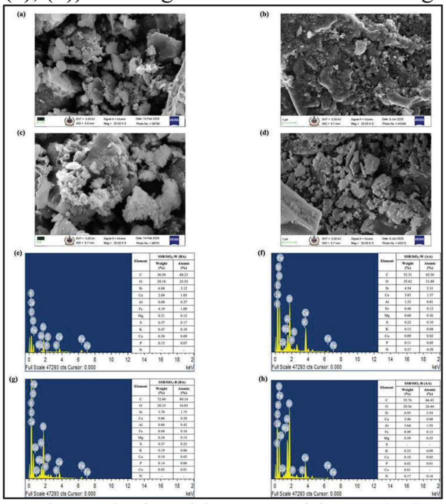

Fig. 2. SEM micrograph of SSB/SiO_2-W, SSB/SiO_2-B adsorbents pre-**(a)**, **(c)**, and post-dye uptake **(b)**, **(d)** recorded at 25.00 KX; EDX mapping of SSB/SiO_2-W, SSB/SiO_2-B adsorbents before-**(e)**, **(g)**, and after RhB decolorization **(f)**, **(h)**.

Fig. 3. (e), **(f)** illustrate the van't Hoff graphs customarily utilized to enumerate the ΔG^o, ΔS^o, and ΔH^o values associated with RhB uptake from effluent solutions using biochar/silica gel composites. Negative ΔG^o, and Positive ΔH^o, and ΔS^o values were ascertained for dye adsorption using both the biochar composites, indicating that the process was spontaneous, and endothermic, accompanied by increasing randomness **(TABLE III.)** [18].

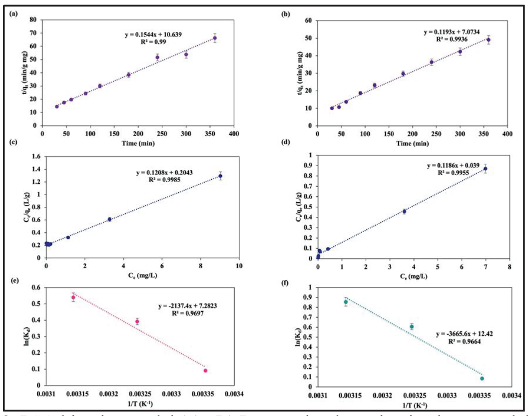

Fig. 3. PSO kinetics model **(a)**, **(b)** Langmuir adsorption isotherm model **(c)**, **(d)**, and thermodynamics profile **(e)**, **(f)** delineating RhB adsorption onto SSB/SiO_2-W, SSB/SiO_2-B adsorbents.

TABLE II. Adsorption kinetics, and isotherm parameters concomitant with RhB uptake from simulated wastewater.

		Parameters	Biochar composites	
			SSB/ SiO_2-W	SSB/ SiO_2-B
Adsorption kinetics	PFO	K_1 (min^{-1})	0.0052	0.0084
		q_e (empirical) (mg/g)	6.5502	7.5180
		q_e (theoretical) (mg/g)	5.0505	6.1595
		R^2	0.9446	0.8679
	PSO	K_2 (g/ (mg.min))	0.0022	0.0018
		q_e (theoretical) (mg/g)	6.4767	8.3822
		q_e (empirical) (mg/g)	6.5502	7.5180
		R^2	0.99	0.9936
Adsorption isotherms	Langmuir	R^2	0.9985	0.9955
		K_L (L/mg)	0.5913	3.0410
		q_m (mg/g)	8.2781	8.4317
	Freundlich	1/n	0.7770	0.5156
		R^2	0.9724	0.9614
		K_F (L/mg)	2.2705	3.9809

TABLE III. THERMODYNAMICS FACTORS INFLUENCING RHB DISCOLORATION FROM AQUEOUS MATRICES EMPLOYING BIOCHAR/SILICA GEL COMPOSITES.

Biochar type	Temperature	ΔS° (J/mol K)	ΔH° (kJ/mol)	ΔG° (kJ/mol)	Adsorption phenomenon type
SSB/SiO_2-W	25 °C	60.5450	17.7701	-0.2813	Spontaneous, and endothermic dye decolorization process accompanied by increased system randomness.
	35 °C			-0.8668	
	45 °C			-1.4922	
SSB/SiO_2-B	25 °C	103.2580	30.4758	-0.3106	
	35 °C			-1.343	
	45 °C			-2.376	

2) Effect of biochar/silica gel composite dosage and pH

The effect of biochar/silica gel composite concentration, and pH of aqueous phase were examined as these factors were known to significantly influence the dye uptake phenomenon. It was ascertained that with an enhancement in the adsorbent dose from 0.01 to 0.1g, the RhB dye removal efficacies were augmented, with > 99% dye removal at biochar composite doses of 0.1 g **(Fig. 4. (a), (c))**. This was attributable. to the availability of plentiful dye sorption sites at higher adsorbent doses. Contrarily, the adsorption capacity of both the biochar adsorbents were reduced at incremental biochar composite doses due to possible agglomeration of active sorption sites ensuing in an extended diffusion pathway for RhB dye molecules [18]. Moreover, utmost dye removal occurred at acidic pH (pH = 2.0) for both the biochar composites, exhibiting a decrease in the dye removal efficiency from 57.14% to 35.03% for SSB/SiO_2-W **(Fig. 4. (b))**, and from 46.67% to 25.97% for SSB/SiO_2-B **(Fig. 4. (d))**. The adsorption capacity of both the biochar/silica gel composites also decreased at incremental solution pH values. RhB dye has a pK_a value of 3.7, and subsists in the cationic form at solution pH values below 3.7, thereby expediting its entry into the pores of the biochar composite at acidic pH. Contrastingly, at solution pH values higher than 3.7, this dye transforms into its zwitterionic form, which promotes the agglomeration of dye moieties into dimers, obstructing its diffusion into the porous biochar composites [19].

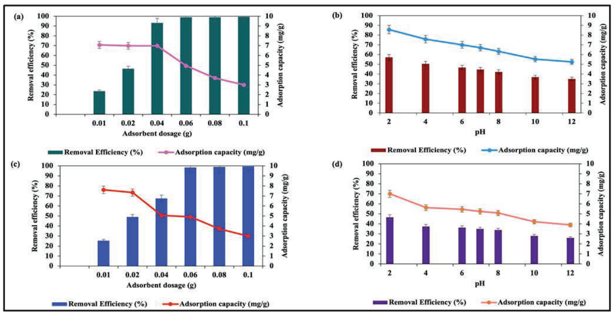

Fig. 4. Impact of **(a)** SSB/SiO_2-W, and **(c)** SSB/SiO_2-B dosage on RhB uptake; Influence of pH of aqueous matrices on dye adsorption using **(b)** SSB/SiO_2-W, and **(d)** SSB/SiO_2-B adsorbents.

3) Comparison with other adsorbents for RhB removal reported in literature

TABLE IV. represents the comparative analysis of SSB/silica gel composites towards RhB uptake from simulated wastewater, alongside various adsorbents reported in literature. SSB/SiO_2-W, and SSB/SiO_2-B composites exhibited better maximal adsorption capacities than some of the adsorbents outlined in previous research. Furthermore, the adsorption process conditions associated with dye removal varied across the studies, and the dye adsorption capacity could be further augmented by conducting batch adsorption studies at elevated concentrations.

TABLE IV. BENCHMARKING RHB REMOVAL PERFORMANCE OF SSB/SiO_2 COMPOSITES AGAINST CONVENTIONAL ADSORBENTS.

Sr. No.	Adsorbent	Preliminary dye concentration (ppm)	Maximal adsorption capacity, q_m (mg/g)	Reference
1.	Biochar derived from coconut fruit shell	100-350	8.1	[10]
2.	Corn stalk activated carbon (treated with phosphoric acid (H_3PO_4))	10-50	5.6	[13]
3.	Orange peel biochar	20-60	3.23	[14]
4.	Australian natural zeolite	0.479- 4.790	2.12	[22]
5.	SSB/SiO_2-W	0.14-15	8.28	Current work
6.	SSB/SiO_2-B	0.14-15	8.43	Current
				work

C. Desorption and regeneration analysis

In order to test the reusability of the dye-loaded biochar In order to test the reusability of the dye-loaded biochar composite adsorbents for subsequent dye adsorption applications, regeneration studies were performed over three cycles using ethanol as the eluent. RhB removal efficacy curtailed from 75.24% to 51.69% for SSB/SiO_2-W, and from 76.27% to 54.93% for SSB/SiO_2-B over three regeneration cycles. The reduction in dye removal efficacy over three regeneration cycles could be ascribed to the prior-desorption process, which dissolved certain components of the biochar composite, thereby modifying its surface characteristics and subsequently ensuing in impediment of the active sorption sites of the biochar composite **(Fig. 5)**.

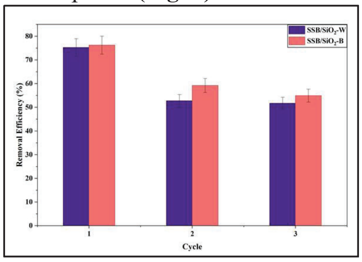

Fig. 5. Cyclic adsorption-desorption experiments of RhB-saturated biochar silica/gel composites.

D. FA-ANN based optimization for forecasting RhB adsorption

In the current research, we have employed the Levenberg Marquardt (LM) Backpropagation Algorithm to train the Artificial Neural Network (ANN), and prognosticate RhB adsorption capacity employing the biochar/silica gel composites. During the ANN modelling process, the number of hidden layer neurons was estimated via the Firefly Algorithm. The ideal neural network configuration for prognosticating RhB discoloration using SSB/SiO_2-W, and SSB/SiO_2-B adsorbents were ascertained to be 5-6-1, and 5-3-1, respectively (5: Neurons in input layer, 6/3: Hidden layer neurons, 1: Neurons in output layer) **(Fig. 6.)**. The models were run multiple times with different initializations, and the best-performing ANN networks were selected to ensure high R^2 and low error values.

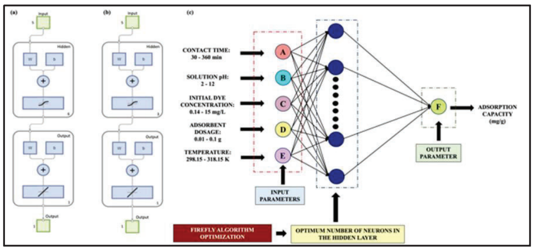

Fig. 6. Optimal ANN topology for predicting RhB discoloration utilizing **(a)** SSB/SiO_2-W, and **(b)** SSB/SiO_2-B adsorbents; **(c)** ANN configuration manifesting input, hidden and output layer.

The ANN parity plots for prognosticating RhB adsorption capacity values for distinct, and overall datasets utilizing the biochar composite adsorbents yielded R^2 values (**All:** SSB/SiO_2-W: 0.9955, SSB/SiO_2-B: 0.9917) close to unity **(Fig. 7 (a), (b))**. Furthermore, correlation coefficient (R) values attained for predicting RhB uptake from simulated wastewater also neared one (Overall: SSB/SiO_2-W:0.9892, SSB/SiO_2-B: 0.9811), implying that the generated ANN model was capable of efficaciously learning, and prognosticating dye adsorption capacity values employing biochar/silica gel composites **(Fig. 7. (c), (d))**. The individual, and overall error values observed for forecasting RhB adsorption capacities using both the biochar composites were low, with the MSE, MAE, and RMSE values all being less than one **(TABLE V.)**. Performance was consistent across training, validation, and testing datasets (SSB/SiO_2-W: R^2 = 0.9785-0.9848; SSB/SiO_2-B: R^2 = 0.9682-0.9743), confirming the models' reliable generalization beyond the training data. The acquisition of R^2, R values nearing unity, along with minimal error values in the generated ANN model substantiates a robust correlation between the experimental, and ANN forecasted values. This ANN model can be efficaciously used for prognosticating adsorption performance across any operating conditions spanning within the empirical limits. From the MSE performance graph it can be noticed that there was a reduction in the MSE values at incremental epoch, with best validation performance observed at 0.3066, and 0.5236 epoch 13, and 8, respectively for SSB/SiO_2-W, and SSB/SiO_2-B adsorbents **(Fig. 7. (e), (f))**. The MSE values attained for the biochar/silica gel composites spanned within the acceptable error limits. The ANN model prognosticated optimal conditions which yielded the highest adsorption capacities for both the biochar composite adsorbents are:- preliminary dye concentration (15 mg/L), contact time (360 minutes), pH (4.74), solution temperature (318.15 K), biochar composite dose (0.02 g).

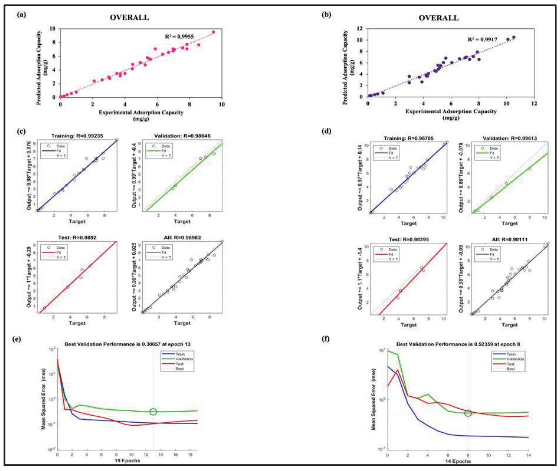

Fig. 7. Parity plots **(a)**, **(b)**, ANN regression plots **(c)**, **(d)**, and MSE performance plots **(e)**, **(f)** for prognosticating RhB adsorption onto SSB/SiO_2-W and SSB/SiO_2-B adsorbents.

TABLE V. STATISTICAL PARAMETERS OF DEVELOPED ANN MODEL FOR PREDICTING RHB UPTAKE ONTO SSB/SILICA GEL ADSORBENTS.

Adsorbent	Statistical parameters	Network Structure	MAE	MSE	RMSE	^{2}	R
	Overall	5-3-1	0.2508	0.1387	0.3724	0.9955	0.9898

SSB/ SiO_2-W	Training		0.1943	0.11	0.3317	0.9848	0.9924
	Validation		0.4852	0.1147	0.3387	0.9731	0.9865
	Testing		0.2766	0.1028	0.3206	0.9785	0.9892
SSB/ SiO_2-B	Overall	5-6-1	0.3952	0.2919	0.5403	0.9917	0.9811
	Training		0.2979	0.1807	0.4251	0.9743	0.9871
	Validation		0.5796	0.4423	0.6651	0.9923	0.9961
	Testing		0.658	0.5717	0.7561	0.9682	0.984

E. Visualization of pearson correlation matrix via heatmap

In this study, the interrelationship between various predictors and responses governing the dye uptake phenomenon using biochar/silica gel composites was evaluated through a correlation matrix heatmap generated using Pearson's correlation coefficient **(Fig. 8. (a), (b))**. A moderately positive and weakly positive correlation between contact time and the adsorption capacities was observed for SSB/SiO_2-W, and SSB/SiO_2-B adsorbents. The solution pH exhibited weakly positive, and negative correlations with the adsorption capacity for SSB/SiO_2-W, and SSB/SiO_2-B adsorbents, respectively. Both the biochar composites demonstrated a strong positive correlation of adsorption capacity with preliminary adsorbate concentration and a weak inverse association with biochar composite dose. Comprehensively, the solution temperature and adsorption capacities of both biochar composites were moderately positively correlated.

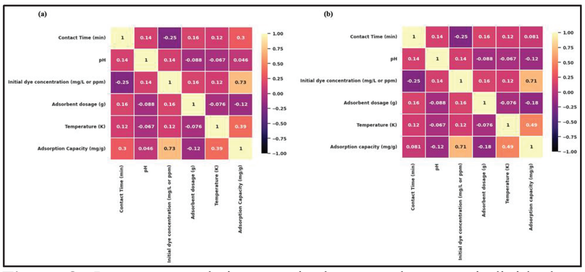

Figure 8: Pearson correlation matrix heatmap between individual, and paired predictors, and responses, for **(a)** SSB/SiO_2-W, and **(b)** SSB/SiO_2-B adsorbents.

IV. CONCLUSION

This work uniquely demonstrates a comparative investigation of SSB functionalized with two distinct grades of silica gel – blue (indicating), and white (non-indicating) for RhB uptake, coupled with FA-optimized ANN Modelling. The synthesized biochar/silica gel composites achieved over 99% RhB removal from simulated effluent solutions at RhB concentrations of 15 ppm. The dye adsorption process was endothermic, spontaneous, and led to an increase in system disorder, following PSO kinetics, and Langmuir isotherms. The plausible mechanisms governing the dye uptake phenomenon included pore-filling, surface complexation, π-π interactions, electrostatic interactions, and hydrogen bonding. The tested RhB dye concentrations were deliberately selected based on Environmental Quality Standards considering maximum permissible limits; however performance in industrial effluents with competing ions may differ, warranting further study. Conclusively, the FA-ANN model effectively prognosticated RhB adsorption capacities and identified the optimal adsorption conditions for both the biochar/silica gel composites.

ACKNOWLEDGMENT

The authors would like to thank Dr. BHVS Narayana Murthy, Vice-Chancellor of DIAT (DU), Pune, for his constant support and motivation.

REFERENCES

[1] K. Naseem, E. Abrar, A. Khalid, M.A. Ismail, Inorganic nanoparticles as a potential catalyst for the reduction of Rhodamine B dye: A critical review, Inorganic Chemistry Communications 163 (2024) 112367.
[2] N. Mayilswamy, A. Nighojkar, M. Edirisinghe, S. Sundaram, B. Kandasubramanian, Sludge-derived biochar: Physicochemical characteristics for environmental remediation, Applied Physics Reviews 10 (2023)
[3] M. He, Z. Xu, D. Hou, B. Gao, X. Cao, Y.S. Ok, J. Rinklebe, N.S. Bolan, D.C.W. Tsang, Waste-derived biochar for water pollution control and sustainable development, Nat Rev Earth Environ 3 (2022) 444–460.
[4] Y. Sakamoto, M. Kaneda, O. Terasaki, D.Y. Zhao, J.M. Kim, G. Stucky, H.J. Shin, R. Ryoo, Direct imaging of the pores and cages of three-dimensional mesoporous materials, Nature 408 (2000) 449–453.
[5] J. Jawad, A.H. Hawari, S. Javaid Zaidi, Artificial neural network modeling of wastewater treatment and desalination using membrane processes: A review, Chemical Engineering Journal 419 (2021) 129540.
[6] K. Sotiriou, N. Supanchaiyamat, T. Jiang, I. Janekarn, A.M. García, V.L. Budarin, D.J. MacQuarrie, A.J. Hunt, Synthesis and application of tuneable carbon–silica composites from the microwave pyrolysis of waste paper for selective recovery of gold from acidic solutions, RSC Adv. 10 (2020) 25228–25238.
[7] L. Chen, B. Mi, J. He, Y. Li, Z. Zhou, F. Wu, Functionalized biochars with highly-efficient malachite green adsorption property produced from banana peels via microwave-assisted pyrolysis, Bioresource Technology 376 (2023) 128840.
[8] J. Wang, X. Guo, Adsorption kinetic models: Physical meanings, applications, and solving methods, Journal of Hazardous Materials 390 (2020) 122156.
[9] M.A. El-Nemr, M. Yılmaz, S. Ragab, M.A. Hassaan, A. El Nemr, Isotherm and kinetic studies of acid yellow 11 dye adsorption from wastewater using Pisum Sativum peels microporous activated carbon, Sci Rep 13 (2023) 4268.
[10] J. Wang, X. Guo, Adsorption isotherm models: Classification, physical meaning, application and solving method, Chemosphere 258 (2020) 127279.
[11] A. Nighojkar, S. Pandey, M. Naebe, B. Kandasubramanian, W.W. Soboyejo, A. Plappally, X. Wang, Using machine learning to predict the efficiency of biochar in pesticide remediation, Npj Sustain. Agric. 1 (2023) 1.
[12] L. Liu, X. Yang, S. Ahmad, X. Li, C. Ri, J. Tang, R.M. Ellam, Z. Song, Silicon (Si) modification of biochars from different Si-bearing precursors improves cadmium remediation, Chemical Engineering Journal 457 (2023) 141194.
[13] T. Jiang, V.L. Budarin, P.S. Shuttleworth, G. Ellis, C.M.A. Parlett, K. Wilson, D.J. Macquarrie, A.J. Hunt, Green preparation of tuneable carbon–silica composite materials from wastes, J. Mater. Chem. A 3 (2015) 14148–14156.
[14] I.H. Nurwahid, M. Khalil, R.T. Yunarti, The enhancement of specific capacitance of carbon derived from spent coffee grounds with SiO2 nanoparticles, Chem. Pap. 77 (2023) 1669–1681.
[15] P. Ghorbannezhad, G. Shen, I. Ali, Microwave-assisted hot water treatment of sugarcane bagasse for fast pyrolysis, Biomass Conv. Bioref. 13 (2023) 14425–14432.
[16] J. Zhang, B. Huang, L. Chen, Y. Li, W. Li, Z. Luo, Characteristics of biochar produced from yak manure at different pyrolysis temperatures and its effects on the yield and growth of highland barley, Chemical Speciation & Bioavailability 30 (2018) 57–67.
[17] J. Wang, Y. Tan, H. Yang, L. Zhan, G. Sun, L. Luo, On the adsorption characteristics and mechanism of methylene blue by ball mill modified biochar, Sci Rep 13 (2023) 21174.
[18] L. Chen, B. Mi, J. He, Y. Li, Z. Zhou, F. Wu, Functionalized biochars with highly-efficient malachite green adsorption property produced

from banana peels via microwave-assisted pyrolysis, Bioresource Technology 376 (2023) 128840.

[19] H.M.H. Gad, A.A. El-Sayed, Activated carbon from agricultural by-products for the removal of Rhodamine-B from aqueous solution, Journal of Hazardous Materials 168 (2009) 1070–1081.

[20] R.T. Kapoor, M. Rafatullah, M.R. Siddiqui, M. Alam, Adsorptive potential of coconut fruit shell biochar as low-cost adsorbent for sequestration of rhodamine B dye: kinetics, thermodynamics and phytotoxicity studies, Biomass Conv. Bioref. (2024).

[21] S.A. Mousavi, B. Kamarehie, A. Almasi, M. Darvishmotevalli, M. Salari, M. Moradnia, F. Azimi, M. Ghaderpoori, Z. Neyazi, M.A. Karami, Removal of Rhodamine B from aqueous solution by stalk corn activated carbon: adsorption and kinetic study, Biomass Conv. Bioref. 13 (2023) 7927–7936.

[22] C. Namasivayam, N. Muniasamy, K. Gayatri, M. Rani, K. Ranganathan, Removal of dyes from aqueous solutions by cellulosic waste orange peel, Bioresource Technology 57 (1996) 37–43.

[23] S. Wang, Z. Zhu, Characterisation and environmental application of an Australian natural zeolite for basic dye removal from aqueous solution, Journal of Hazardous Materials 136 (2006) 946–952.